Modeling the Longitudinal Flight Dynamics of a Fixed-Wing Aircraft by using a Multibody System Approach

Carmine Maria Pappalardo, Maria Curcio, Domenico Guida

***Abstract*—Considering the multibody method for the dynamic analysis of mechanical systems, this paper aims at constructing a simple computer model describing the dynamics of a fixed-wing aircraft performing a longitudinal motion. To this end, a simplified model of an aerial vehicle was analyzed without control surfaces, featuring an axial thrust, and having limited aerodynamic actions. By using the Digital DATCOM software, the modeling of the aerodynamic coefficients was then taken into account considering also the elevator as a control surface. First, aircraft dynamics was studied in general in the context of multibody dynamics. Then, the case study considered as the illustrative example of the paper was analyzed, namely the Cessna 172 Skyhawk aircraft. By modeling the externally applied actions and the aerodynamic coefficients, the fundamental mechanics behind the take-off phase of the flight was subsequently analyzed. In the paper, the equations of motion describing the dynamic behavior of the illustrative example were driven using a Lagrangian formulation approach. The dynamic model of the demonstrative example was then implemented in a computer code constructed in the MATLAB environment. By doing so, the goal of this process was to develop as accurately as possible a virtual model of the Cessna 172 Skyhawk aircraft. As shown in the paper using numerical simulations, the computer model of the case study analyzed in this work is able of simulating the vertical motion of the aircraft. In the conclusive part of the manuscript, a discussion about the dynamic behavior of the aircraft found in this investigation and some comments on several topics for future research are reported as well.**

***Index Terms*—Fixed-wing aircraft, longitudinal flight mechanics, multibody systems, Lagrangian dynamics, Cessna 172 Skyhawk, aerodynamic coefficients, MATLAB simulation environment, digital DATCOM software.**

I. Introduction

In this section, background material useful for introducing the issues addressed in this investigation is included. First, a punctual discussion about the significance of the current investigation is provided. Then, a short literature survey is reported in order to inform the readers potentially unaware about some topics elaborated in the paper. Afterward, the scope of the present paper is summarized together with the contributions provided in this investigation. The structure of the manuscript is finally offered to present the content of the entire paper.

Manuscript received June 10, 2022; revised October 18, 2022.

Carmine M. Pappalardo is an Assistant Professor at the Department of Industrial Engineering, University of Salerno, Via Giovanni Paolo II, 132, 84084 Fisciano, Salerno, Italy (corresponding author, email: cpappalardo@unisa.it).

Maria Curcio is a Researcher at the Spin-Off MEID4 s.r.l., Via Giovanni Paolo II, 132, 84084 Fisciano, Salerno, Italy (email: m.curcio16@studenti.unisa.it).

Domenico Guida is a Full Professor at the Department of Industrial Engineering, University of Salerno, Via Giovanni Paolo II, 132, 84084 Fisciano, Salerno, Italy (email: guida@unisa.it).

A. Background Information and Research Significance

Virtual prototyping and dynamic modeling of a mechanical system are important steps in the development of computer-aided design and dynamic analysis [1]–[3]. In fact, the virtual model constructed through the help of computer-aided design and engineering tools allows engineers to analyze the performance of the system of interest before actually manufacturing and using it [4]–[6]. This is especially important in the field of aviation, where system damages carry a very high risk for the integrity of the system itself and, more importantly, for the human lives of the operators and users that interact with the aircraft [7]–[9].

UAV is an acronym for Unmanned Aerial vehicle. It is possible to remotely guide and command this special category of aerial systems by defining offline a feasible flight plan or by using online a ground-based control station [10]–[12]. Compared to a classic aircraft, the main differences are in flight autonomy, communication mechanisms, data management, and avionics [13]–[15]. In the beginning, UAVs were mainly used for military purposes such as reconnaissance missions and military attacks [16]–[18]. In recent years, their use in complex and realistic scenarios has been growing day by day by virtue of their great potential in exploration and monitoring applications. In addition to the capacity of being useful in complex applications, one of the principal features of UAV systems is represented by their low ethical and economical costs [19], [20]. Also, in modern applications, UAVs can serve as assistant robots for performing multiple tasks [21], [22]. Therefore, this large class of flying vehicles that work autonomously is becoming intertwined with robotic applications [23]–[25].

Computer-Aided Design (CAD) and Computer-Aided Engineering (CAE) software have become prominent in the modern engineering age. In particular, a special role is played in this context by Multibody System Dynamics (MBD) [26]–[28], and by advanced multibody simulations based on the concept of the Integration of Computer-Aided Design and Analysis (I-CAD-A) [29]–[31]. While computer-aided design systems are typically employed only for geometry creation, the multibody system software is used for automatically generating and numerically solving the Differential-Algebraic Equations of motion (DAEs) that describe the dynamic behavior of the mechanical system of interest [26], [32], [33]. The possibility of realistically simulating in advance the behavior of a complex machine during the design process

before its actual manufacturing is advantageous since this feature is very useful in engineering and industrial applications.

The concepts described above clarify the background context in which the present investigation is collocated and evidence the importance of the present study, which deals with the multibody modeling in a virtual computational environment of the longitudinal flight dynamics of a simple aircraft.

B. Literature Review

Generally, in the field of flight dynamics, classical Newtonian approaches are commonly utilized to obtain the dynamic equations of an aircraft [8], [34], [35]. For example, Schmidt proposed the use of linear algebra principles to mathematically formulate the dynamical equations of an aircraft [36]. In some particular applications, blended Newtonian and Lagrangian procedures are employed to realize these types of dynamic analyses [37], [38]. An alternative way to predict the flight path of an aircraft during its motion is presented by Peyada and Gosh [39]. By using a feedforward neural network, they developed a method capable of timely predicting the system performance of their aircraft model. On the other hand, both the works of Thelander and Sinha provide a comprehensive overview of these processes by using Newton second law [7], [9], [40]. In this vein, Mukherjee and Sinha carried out the computer simulation and the optimal control of a combat aircraft system having six degrees of freedom [41].

After having mathematically obtained the dynamical model of an aircraft, one can create the corresponding dynamical model in MATLAB. This is aimed at performing virtual simulations of the system performance during the flight considering realistic maneuvers [42]. For instance, the works by Tu and Lin [43], as well as the work of Yang and Yuan [44], explored these topics. In [45], Mukherjee and Sinha also studied the dynamics and control of aircraft performing complex maneuvers. Rao and Sinha studied the critical problem concerning the spin motion of aircraft and proposed a nonlinear sliding mode controller to address this issue [46]. In [47], Trachte et al. performed dynamical simulations of a multi-rotor aircraft and analyzed its control problem by using a predictive control strategy. In [48], Harikumar et al. studied by performing dynamical simulations multi-unmanned aerial vehicles that were specifically designed to seek and destroy a moving target having complex dynamics, like a forest fire. Another important topic related to the dynamic analysis of aircraft is the system identification of airplane models that leverages the measurement of input-output data [49], [50]. To this end, Hamel and Botez identified a dynamic model of the Cessna Citation X business airplane from real flight test data [51]. Sinha et al. proposed a mathematical technique arising from the use of neural partial differentiation to address the numerical issues encountered when dealing with unstable aircraft dynamics and the problem of the estimation of their parameters [52].

To study the kinematics and dynamics of an articulated system, multibody modeling is a very suitable tool [26]. Several papers found in the literature focused on the issues concerning the dynamics of multibody mechanical systems underline the interest and complexity of the topic considered in this work [53]–[58]. The systematic modeling approach based on the dynamics of multibody systems can be successfully utilized in the field of flight dynamics as well [59]–[61]. In this vein, the first and foremost step is fundamentally represented by the proper use of rigid bodies for modeling and describing aircraft systems, thereby considering applied on them the driving forces and the control inputs as external actions [62], [63]. In effect, all the external actions applied on the aircraft should be analyzed in their own frame of reference [30]. It is also important to project the forces in the absolute frame of reference, which represents the unique common metric of the entire analysis. The combined use of multibody and Lagrangian approaches can be considered a valid, effective, and efficient alternative procedure for the study of all mechanical systems, including the system under investigation [29], [64]. As discussed in this work, the multibody method for the kinematic and dynamic analysis of rigid mechanical systems can be also utilized to study longitudinal flight dynamics of aircraft [65]. Aircraft can be modeled as a multibody system, in which each single component is connected to the system by mechanical joints. By the addition of a specific term in the dynamical model each rigid body, representing joint connections, a multibody flight dynamics model can be built and the dynamical model can be constructed. This is the fundamental approach followed in this research study.

C. Scope and Contributions of this Study

In this paper, an investigation of all the mechanisms and the basic principles behind flight dynamics is proposed. This is a preliminary work that starts from the study of aircraft dynamics, then arrives at the modeling of all the relevant actions acting on the system under consideration. The fundamental objective of this study is to devise a simplified strategy that allows for the mathematical determination of the dynamical equations of the aircraft and then to predict the first phase of the flight through a dynamic simulation. This is done by utilizing numeric computations and symbolic calculations in a general-purpose program based on the MATLAB simulation environment, in which the system dynamic model is symbolically generated and, subsequently, numerically solved through the use of effective computational procedures, leading to a set of dynamical simulations for the demonstrative model of interest for this work.

In this research, a computer model for the simulation in MATLAB of the dynamic performance of an aircraft during one of the most important phases of its flight is developed, that is, the take-off of a small aircraft is analyzed in the context of of multibody system dynamics. Thus, the multibody approach is used to model the aircraft as a rigid body and to obtain its set of equations of motion [66]–[68]. By doing so, and considering only the longitudinal flight dynamics, the aircraft of interest is mathematically described in its longitudinal plane as a multibody mechanical system having three degrees of freedom. Preliminary assumptions and simplifying hypotheses are unavoidably considered to achieve this goal, namely, the hypotheses of a simplified set of aerodynamic actions, an axial thrust force, and the

presence of the elevator as the main control surface are taken into account. These simplifying assumptions will be gradually removed in future investigations.

In order to validate the physical coherence with the expected performance of the computational results obtained from the computer simulations accomplished by implementing in MATLAB the proposed dynamical equations, the Cessna 172 Skyhawk is assumed as the demonstrative example of this investigation [69]. The Cessna 172 Skyhawk is manufactured since the fifties by the American firm called Cessna Aircraft Company. This is one of the most widely produced aircraft to date [70]. Since the design data for Cessna 172 Skyhawk are available on the internet with no economic costs, it was chosen to carry out a systematic analysis of the computational results derived from the computer simulations arising from the numerical solution of the dynamic model of this aircraft devised in this work. In particular, a realistic set of aerodynamic coefficients pertaining to this aircraft considered in the case study were obtained by using the digital DATCOM software that is freely available on the internet. The performance behavior found for the aircraft system assumed as the illustrative example of this investigation is consistent with the physical features of the problem under consideration.

D. Organization of the Manuscript

Apart from Section I, which reports an introductory discussion about the main topics addressed in the current work, this manuscript is organized as follows. In Section II, the system of interest for this research work is modeled. This is done by studying the kinematics and dynamics of the aircraft as a rigid system together with the modeling of aerodynamic actions. In Section III, the numerical results of the dynamic simulations conducted by implementing the dynamical model devised in this work using MATLAB together with DATCOM are shown and discussed. Finally, Section IV focuses on the conclusions drawn in this study and provides a proposal for future developments related to the present investigation.

II. Kinematic and Dynamic Analysis of Multibody Systems, Elements of Flight Mechanics, and Basics of Aerodynamics Modeling

This section discusses the principal mechanical features concerning the kinematics and dynamics of articulated systems, which can be described as multibody systems, and provides some basic elements of flight mechanics. More precisely, the analytical tools belonging to the dynamics of multibody mechanical systems are utilized for mathematically describing the aircraft system representing the main object of this paper. This is done by modeling the case study of this research as a rigid body subjected to force fields, while the basic concepts and techniques taken from the flight mechanics are employed to properly define the aerodynamic actions applied on the aircraft. This section, therefore, provides the fundamental background material essential for the development of the dynamic equations investigated in the present paper.

A. Elements of Multibody System Dynamics

A key mechanical concept of multibody dynamics is the identification of the number of degrees of freedom of a given articulated system, which is essentially the total number of independent parameters that allows for unambiguously describing the geometric configuration in the space of the system of interest [71], [72]. A rigid body in a two-dimensional space has three degrees of freedom, two related to translation and one related to rotation around the perpendicular axis. Similarly, a rigid body in a three-dimensional space is endowed with six degrees of freedom, three translational degrees of freedom associated with the displacement of its center of mass and three rotational degrees of freedom which define the orientation of a body-fixed reference frame with respect to an absolute reference system.

Multibody systems consist of mutually connected rigid and deformable components or bodies [73], [74]. For instance, aerospace and automotive systems, as well as articulated systems in general, are mechanical systems that can be imagined as formed by a set of components, which can be rigid or flexible, held together by mechanical constraints, such as revolute joints, prismatic joints, spherical joints, and so on. These systems also undergo the dynamic influence of force elements and force fields of various nature, such as springs, dampers, actuators, etcetera. The movements of the parts that form of an entire mechanical system modeled as a multibody system can be studied by analyzing the interactions between the single elements that form its structure. To this end, the differential equations describing the motion can be derived utilizing the classical Newtonian approach or by using the Lagrangian formalism.

The set of Lagrange equations of the first and the second kind represents a viable technique for the mathematical generation of the equations of motion of complex multibody mechanical systems [75], [76]. Given the number of degrees of freedom of the system indicated by n, one needs n ordinary differential equations to describe the motion, which turns out to typically be nonlinear. To this end, assume the system vector of Lagrangian coordinates denoted as:

$$\mathbf{q} = \begin{bmatrix} q_1 & q_2 & \dots & q_k & \dots & q_n \end{bmatrix}^T \tag{1}$$

The set of Lagrange equations, associated with the minimal set of generalized coordinates introduced above, is given by:

$$\frac{d}{dt}\left(\frac{\partial T}{\partial \dot{q}_k}\right) - \frac{\partial T}{\partial q_k} + \frac{\partial U}{\partial q_k} = Q_k, \quad k = 1, 2, ..., n \tag{2}$$

where U is the system potential energy and T is the system kinetic energy. In the Lagrangian formulation, the mechanical component associated with the force element/field applied to the degree of freedom k is denoted with Q_k and is given by:

$$Q_k = \sum_{j=1}^{N_a} \mathbf{F}_j \frac{\partial \mathbf{r}_j}{\partial q_k} \tag{3}$$

where $\mathbf{F}_j = \begin{bmatrix} F_{x,j} & F_{y,j} & F_{z,j} \end{bmatrix}^T$ stands for an external force of the multibody system, generically acting on the rigid body labeled with the integer number j, that affects the system degree of freedom labeled with k, and N_a is another integer number representing the number of externally applied

forces.

To correctly define the mathematical form of the system kinetic and potential energy, as well as of the vector of generalized external forces, an important analytical step is the kinematic analysis. For this purpose, the relationships between the remarkable points of the system are identified by applying the following geometric relation:

$$\mathbf{r}_j(P) = \mathbf{R}_j + \mathbf{A}_j \bar{\mathbf{u}}_j(P) \tag{4}$$

where $\mathbf{r}_j(P)$ is the absolute position vector of a generic material point P belonging to a generic rigid body j, $\mathbf{R}_j$ is the global position vector of the centroid of a generic rigid body j, $\mathbf{A}_j$ is the rotation matrix that identifies the spatial orientation of the generic rigid body j, and $\bar{\mathbf{u}}_j(P)$ is the position vector of a generic material point P defined with respect to the body-fixed reference frame of the body j.

Knowing the positions concerning the global reference system, the corresponding velocities are derived, thereby allowing for the definition of the kinetic and potential energies. Assuming a body-fixed reference system collocated at the centroid, the kinetic energy T_j of a rigid body j is given by:

$$T_j = T_{t,j} + T_{r,j} = \frac{1}{2} m_j v_j^2 + \frac{1}{2} I_{O,j} \omega_j^2 \tag{5}$$

where $T_{t,j}$ is the translational kinetic energy of the rigid body j, $T_{r,j}$ is the rotational kinetic energy of the rigid body j, v_j is the magnitude of the linear velocity of the center of mass of the rigid body j, ω_j is the magnitude of the angular velocity of the rigid body j, m_j is the total mass of the rigid body j, and $I_{O,j}$ is the mass moment of inertia of the rigid body j referred to the point O. The potential energy U_j of a rigid body j, collocated in a constant gravitational field defined by the gravity acceleration g, is given by:

$$U_j = m_j g h_j \tag{6}$$

where h_j represents the altitude of the centroid of the rigid body j collocated in the gravity field. Furthermore, the Lagrangian component vector $\mathbf{Q}_{e,nc}$ can be readily determined by calculating the partial derivative of the virtual work $\delta W_{e,nc}$ of the nonconservative forces computed with respect to the virtual displacement of the Lagrangian coordinate set $\delta\mathbf{q}$. Thus, one can write:

$$\mathbf{Q}_{e,nc} = \left(\frac{\delta W_{e,nc}}{\delta \mathbf{q}} \right)^T \tag{7}$$

By carefully conducting the mathematical derivation mentioned above, the set of Lagrange equations of the second kind can be systematically employed to find the differential equations of motion. Since this is an error-prone process, a computational procedure to find the aircraft dynamical model is developed in the paper, and this is done through symbolic computation carried out in MATLAB.

B. Fundamentals of Flight Mechanics

The goal of this subsection is to demonstrate how the fundamental elements of flight mechanics were employed in this investigation to derive the aircraft aerodynamic actions within the multibody dynamics computational framework [7], [9].

The incidence of an air flow on the wing allows the aircraft to remain in flight. This flow is deflected downward by the wings. Therefore, because of the presence of a difference in the values of the pressure between the upper and the lower surfaces of the airfoil, the aircraft is subjected to an upward thrust force [77].

Assuming, for simplicity, a flat earth surface, to consistently construct a reliable model of a simplified aircraft, one needs to introduce three different reference systems [36]. The first frame of reference is an earth-fixed reference system considered as the absolute inertial reference frame and indicated by the symbols $\left(O^E, X^E, Y^E, Z^E\right)$, with its origin typically collocated on the earth surface and having its Z^E axis directed to the center of the earth. For simplicity, the earth-fixed reference frame is assumed as the inertial system of reference that is employed as the absolute reference system. The second reference frame is the body-fixed reference frame indicated by the symbols $\left(G, X^B, Y^B, Z^B\right)$, which is utilized to identify instant by instant the absolute position and the absolute orientation of the aircraft with respect to the earth-fixed axis system. In the body-fixed frame of reference, G is the centroid of the aircraft under consideration, X^B is the axis directed to the front of the aircraft, and Z^B is the axis taken perpendicular to the axis X^B. By doing so, the plane X^BZ^B represents the plane of symmetry of the entire system. The third frame of reference is the wind-fixed reference frame indicated by the symbols $\left(G, X^W, Y^W, Z^W\right)$, which is utilized to conveniently project the aerodynamic actions. In the wind-fixed reference system, X^W is the axis pointing towards the relative direction of the wind, while Z^W is the axis that is taken normal to the axis Z^W and lies in the plane of symmetry of the system.

The proper geometric definition of the body-fixed, earth-fixed, and wind-fixed reference systems represents a preliminary step of paramount importance for the identification of the fundamental aerodynamic forces and moments required for the use and the implementation of the flight mechanics concepts. More specifically, the knowledge of the angle of attack denoted with α is crucial in this type of investigation. In fact, it affects the aerodynamic actions of the aircraft [78], [79]. It is constructed by measuring the angle between the longitudinal axis of the rigid body representing the aircraft system and the absolute direction of the relative velocity of the wind that runs over the airfoil. Therefore, it represents the angular distance between the axes X^B and X^W. By following the typical convention, one can identify a negative value of the angle of attack when the lift force that affects the airfoil is in the upper-lower direction of the airfoil and positive vice versa. It is, therefore, calculated as follows:

$$\alpha = \tan^{-1}\left(\frac{w}{u}\right) \tag{8}$$

where, as shown in Figure 1, w and u denote the third and the first component of the velocity vector, respectively.

In general, for correctly modeling the spatial motion of an aircraft, one should take into account three principal categories of aerodynamic actions affecting this system. These are the force induced by the aerodynamic actions, the force of gravity, and the force of propulsion. The force induced by the aerodynamic actions is indicated by the symbol $\mathbf{F}_A$ and acts along the relative direction of the wind velocity in the wind-fixed frame of reference [80], [81]. The force of

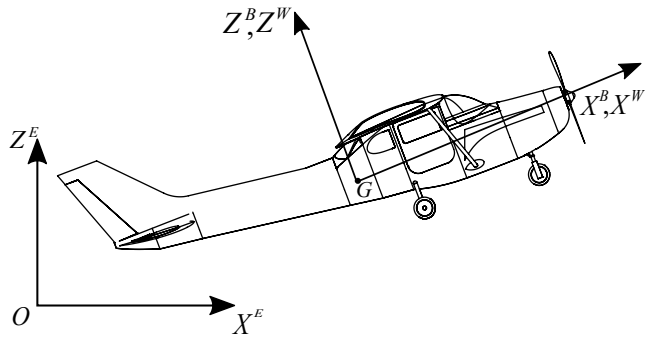

Fig. 1. Aircraft model and reference systems.

gravity is indicated by the symbol $\mathbf{F}_G$ and acts along the vertical axis of the earth-fixed frame of reference. The force of propulsion is indicated by the symbol $\bar{\mathbf{F}}_P$ and acts along a predetermined constant direction in the body-fixed frame of reference. If one considers only the longitudinal motion of an aircraft, the set of externally applied forces mentioned before can be analytically described as the following:

$$\mathbf{F}_G = \begin{bmatrix} 0 \\ mg \end{bmatrix}_E \tag{9}$$

$$\bar{\mathbf{F}}_P = \begin{bmatrix} T_{p,x} \\ 0 \end{bmatrix}_B \approx \begin{bmatrix} T_p \\ 0 \end{bmatrix}_B \tag{10}$$

$$\mathbf{F}_A = \begin{bmatrix} -D \\ -L \end{bmatrix}_W = \begin{bmatrix} -D\cos(\alpha) + L\sin(\alpha) \\ -D\sin(\alpha) - L\cos(\alpha) \end{bmatrix}_B \tag{11}$$

where m is a constant quantity denoting the total mass of the aircraft, g identifies the constant gravity acceleration, T_p is a function of time describing the propulsion force generated by the engines of the aircraft, L is a function of the aircraft configuration representing the magnitude of the lift force, and D is a function of the aircraft configuration representing the magnitude of the drag force. One can also define the aerodynamic actions as follows:

$$L = \frac{1}{2}\rho v_\infty^2 S C_L \tag{12}$$

$$D = \frac{1}{2}\rho v_\infty^2 S C_D \tag{13}$$

where C_L is a constant parameter representing the lift coefficient, C_D is a constant parameter representing the drag coefficient, ρ is a constant parameter representing the density of the air, v_∞ is a function of the aircraft configuration representing the relative velocity of the aircraft, and S is a constant parameter representing the reference surface [7], [9]. Additionally, one can also introduce the net moment applied to the aircraft, which is referred to as the pitching moment, it is calculated about the Y^B axis of the body-fixed reference frame, and it is mathematically given by the following equation:

$$M_m = \frac{1}{2}\rho v_\infty^2 S c C_m \tag{14}$$

where C_m is a constant parameter representing the pitching moment coefficient and c is another constant coefficient representing the mean aerodynamic chord [7], [9].

C. Modeling the Aerodynamic Coefficients

Generally, in the literature, the aerodynamic coefficients are modeled in what is called a quasi-steady approach [7], [9]. By doing so, these coefficients are functions only of flight variables at a generic instant of time, not of those at previous instants of time. The aerodynamic forces can, therefore, be modeled as the sum of four different aerodynamic effects and are given by:

$$\begin{aligned} C_k(t) = {} & C_{k,\text{static}}(\text{Ma}, \alpha, \beta, \delta) \\ & + C_{k,\text{dynamic}}\left(\tfrac{(p_b - p_w)b}{2V}, \tfrac{(q_b - q_w)c}{2V}, \tfrac{(r_b - r_w)b}{2V}\right) \\ & + C_{k,\text{flow}}\left(\tfrac{p_w b}{2V}, \tfrac{q_w c}{2V}, \tfrac{r_w b}{2V}\right) \\ & + C_{k,\text{downwash}}(\alpha(t-\tau), \beta(t-\tau)) \end{aligned} \tag{15}$$

where C_k represents a generic aerodynamic coefficient labeled with the subscript k. In Equation (15), all variables are evaluated at the same time t, except where explicitly mentioned. The static term denoted with $C_{k,\text{static}}$ depends on the Mach number Ma of the relative flow, as well as the aerodynamic angles α and β, and the control surface deflection δ. The dynamic term $C_{k,\text{dynamic}}$ depends on the three components of the relative angular velocities between the body-fixed axes and the wind-fixed axes, which are respectively denoted with the six scalar functions p_b, q_b, r_b, p_w, q_w, and r_w. The third term denoted with $C_{k,\text{flow}}$ is the flow curvature effect, which arises when the aircraft is flying following a curved path. It is a function of the angular velocity components corresponding to the nondimensional wind-axis, which represent the flight path curvature. The downwash lag term denoted with $C_{k,\text{downwash}}$, on the other hand, is the only term that is strictly not a quasi-steady effect as it represents the aerodynamic forces/moments generated at the tail due to changes in α and β at the wing at an earlier time equal to $\tau \approx \frac{l_t}{V}$, where l_t represents the distance between the aerodynamic center of the tail and the wing. It is noteworthy to emphasize the fact that proper modeling of the aerodynamic coefficients relative to the aircraft of interest is of fundamental importance for obtaining from dynamical simulations a set of numerical results that is coherent with the physics of the problem under study.

III. Numerical Results and Discussion

This section focuses on the description of the aircraft model developed and analyzed in this paper. The first subsection contains a concise illustration of the main properties of the demonstrative example analyzed in the paper. In the second subsection, the simplifying assumptions that characterize the case study, such as the absence of control surfaces, the consideration of an axial thrust force, and the aircraft modeling including a basic set of aerodynamic actions, are described. In the third subsection, the case of an aircraft with more realistic aerodynamics is considered, as well as the presence of the elevator as the only control surface. Finally, a general discussion of the numerical results obtained through computer simulations is provided in the fourth subsection.

Once the system is modeled by employing a Lagrangian

approach, the dynamical equations are symbolically derived and transformed in numerical procedure using MATLAB in a quasi-automatic process. Thus, this section includes the description of the case study, the numerical results calculated by using the approach proposed in the paper, and a discussion of the findings of the paper.

A. Description of the Case Study

In this subsection, the illustrative system of interest for this research work is introduced and described in detail to simplify the successive process of integration between the computer-aided design and analysis [82], [83]. A list of all system data is reported in Table I.

TABLE I
CESSNA 172 SKYHAWK MAIN FEATURES.

Parameters	Data (Units)
Length	8.28 (m)
Wingspan	11.0 (m)
Height	2.72 (m)
Wing area	16.2 (m^2)
Aspect ratio	7.32 (−)
Airfoil type	NACA 2412
Empty weight	767.0 (kg)
Gross weight	1111.0 (kg)
Takeoff distance	290.0 (m)
Rate of climb	3.66 (m/s)
Cruise velocity	226.0 (km/h)
Stall velocity	87.0 (km/h)
Mean aerodynamic chord	1.47 (m)
Lift coefficient	0.147 (−)
Drag coefficient	0.019 (−)
Pitching moment coefficient	0 (−)
Moment of inertia	1824.93 (kg × m^2)

To derive a mechanical model of the demonstrative system considered as the case study of this paper, a single rigid body is used to model the dynamical behavior of the aircraft. For this purpose, three degrees of freedom were taken into account. Among the three system degrees of freedom, the first two of them represent the translation of the center of mass of the aircraft, whereas the third and last one represents the rotational motion of the aircraft in the longitudinal plane. Therefore, a set of three Lagrangian coordinates, two for the translation (x and z) and one for the rotation about the axis orthogonal to the plane considered for the motion (θ), is chosen. The generalized coordinate vector of the mechanical model under study is given by:

$$\mathbf{q} = \begin{bmatrix} x & z & \theta \end{bmatrix}^T \tag{16}$$

where x and z identify the horizontal and vertical coordinates of the aircraft center of mass, respectively, θ is the angular displacement of the aircraft longitudinal axis, $d = 2$ is the space dimension, and $n_q = 3$ is the number of Lagrangian coordinates. Once the dimensions d and n_q are set, one can determine the number of state variables as $n_z = 2n_q = 6$, which will be employed in the standard definition of the state-space dynamic model introduced in the computer implementation of the numerical integration algorithm.

To simplify the geometric representation of the system at hand, the geometry aircraft is simply modeled as a triangle. The vertices of the triangular geometric shape used to model the aircraft are denoted by the three points A, B, and C, as shown in Figure 2.

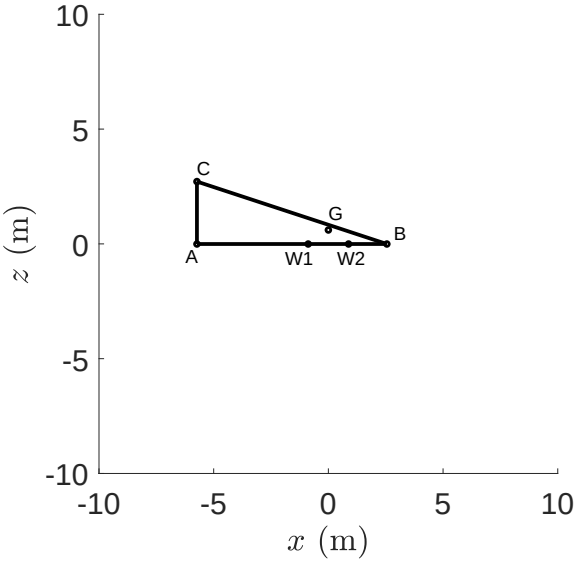

Fig. 2. System geometry schematization.

The geometric points W_1 and W_2 shown in Figure 2 serve to identify the wheels of the aircraft, while the point G represents the centroid of the aircraft. Three fundamental reference systems are introduced, as discussed in the previous subsection. The geometric vectors of the relevant geometric points $\mathbf{r}_A$, $\mathbf{r}_B$, and $\mathbf{r}_C$ can be respectively derived by applying the fundamental formula of rigid kinematics as follows:

$$\begin{aligned}\mathbf{r}_A &= \mathbf{R}_{CM} + \mathbf{A}_{be}\bar{\mathbf{u}}_A \\ &= \begin{bmatrix} x \\ z \end{bmatrix} + \begin{bmatrix} \cos(\theta) & -\sin(\theta) \\ \sin(\theta) & \cos(\theta) \end{bmatrix} \begin{bmatrix} -(B_a - x_{CG}) \\ -z_{CG} \end{bmatrix} \\ &= \begin{bmatrix} x - (B_a - x_{CG})\cos(\theta) + z_{CG}\sin(\theta) \\ z - z_{CG}\cos(\theta) - (B_a - x_{CG})\sin(\theta) \end{bmatrix}\end{aligned} \tag{17}$$

$$\begin{aligned}\mathbf{r}_B &= \mathbf{R}_{CM} + \mathbf{A}_{be}\bar{\mathbf{u}}_B \\ &= \begin{bmatrix} x \\ z \end{bmatrix} + \begin{bmatrix} \cos(\theta) & -\sin(\theta) \\ \sin(\theta) & \cos(\theta) \end{bmatrix} \begin{bmatrix} x_{CG} \\ -z_{CG} \end{bmatrix} \\ &= \begin{bmatrix} x + x_{CG}\cos(\theta) + z_{CG}\sin(\theta) \\ z - z_{CG}\cos(\theta) + x_{CG}\sin(\theta) \end{bmatrix}\end{aligned} \tag{18}$$

$$\begin{aligned}\mathbf{r}_C &= \mathbf{R}_{CM} + \mathbf{A}_{be}\bar{\mathbf{u}}_C \\ &= \begin{bmatrix} x \\ z \end{bmatrix} + \begin{bmatrix} \cos(\theta) & -\sin(\theta) \\ \sin(\theta) & \cos(\theta) \end{bmatrix} \begin{bmatrix} -(B_a - x_{CG}) \\ H_a - z_{CG} \end{bmatrix} \\ &= \begin{bmatrix} x - (B_a - x_{CG})\cos(\theta) - (H_a - z_{CG})\sin(\theta) \\ z + (H_a - z_{CG})\cos(\theta) - (B_a - x_{CG})\sin(\theta) \end{bmatrix}\end{aligned} \tag{19}$$

where $\mathbf{R}_{CM}$ denotes the absolute position vector of the aircraft centroid, $\mathbf{A}_{be}$ identifies the global rotation matrix of the body-fixed coordinate system, x_{CG} and z_{CG} represent the local components corresponding to the Cartesian coordinates of the aircraft center of mass, while B_a is the aircraft base length and H_a is the aircraft height, which respectively represent the lengths of the segments $\overline{AB}$ and $\overline{AC}$ shown in Figure 2. Additionally, one can readily define the absolute velocity vector of the aircraft centroid denoted with $\dot{\mathbf{R}}_{CM}$, consisting of the derivative with respect to the time of the two generalized coordinates. In the computation of this velocity vector, the action of a wind current denoted with $\mathbf{w}$ is also considered. This is done by using two additional quantities, namely, the wind direction indicated as α_W and its intensity indicated as w_0, as described below:

$$\begin{aligned}\dot{\mathbf{R}}_{CM,\text{relative}} &= \dot{\mathbf{R}}_{CM} - \mathbf{w} \\ &= \begin{bmatrix} \dot{x} - w_x \\ \dot{z} - w_z \end{bmatrix} = \begin{bmatrix} \dot{x} - w_0 \cos(\alpha_w) \\ \dot{z} - w_0 \sin(\alpha_w) \end{bmatrix}\end{aligned} \tag{20}$$

The square of the magnitude of the relative wind velocity is indicated as $v^2_{CM,\text{relative}}$ and is given by:

$$\begin{aligned}v^2_{CM,\text{relative}} &= \dot{\mathbf{R}}^T_{CM,\text{relative}} \dot{\mathbf{R}}_{CM,\text{relative}} \\ &= (\dot{x} - w_0 \cos(\alpha_w))^2 + (\dot{z} - w_0 \sin(\alpha_w))^2\end{aligned} \tag{21}$$

The angular velocity of the aircraft modeled as a rigid body is indicated as ω_a and is equal to:

$$\omega_a = \dot{\theta} \tag{22}$$

The time law T_p of the thrust force $\mathbf{F}_P$ is modeled as a ramp function and is given by:

$$T_p = F_t, \quad F_t = \begin{cases} T_{p_c}\left(3\tau^2 - 2\tau^3\right) & , \quad t \le t_{t_c} \\ T_{p_c} & , \quad t > t_{t_c} \end{cases} \tag{23}$$

with:

$$\tau = \frac{t}{t_c} \tag{24}$$

and

$$\begin{aligned}\mathbf{F}_P &= \mathbf{A}_{be} \bar{\mathbf{F}}_P \\ &= \begin{bmatrix} \cos(\theta) & -\sin(\theta) \\ \sin(\theta) & \cos(\theta) \end{bmatrix} \begin{bmatrix} T_p \\ 0 \end{bmatrix} \\ &= \begin{bmatrix} T_p \cos(\theta) \\ T_p \sin(\theta) \end{bmatrix}\end{aligned} \tag{25}$$

where T_{p_c} identifies the final value for the cruise motion of the thrust force and t_c represents the transient time of the ramp function. A graphical representation of the time law T_p of the thrust force is shown in Figure 3.

To model in a simple but effective fashion the contact between the aircraft and the ground, a penalty approach is employed. For this purpose, two penalty forces denoted with $F_{n_{c_1}}$ and $F_{n_{c_2}}$ are applied in the correspondence of the wheels in order to prevent the interpenetration between the aircraft and the ground. The two global vectors of penalty forces acting on the wheels denoted with $\mathbf{F}_{n_1}$ and $\mathbf{F}_{n_2}$ are modeled as described below. The first global force vector

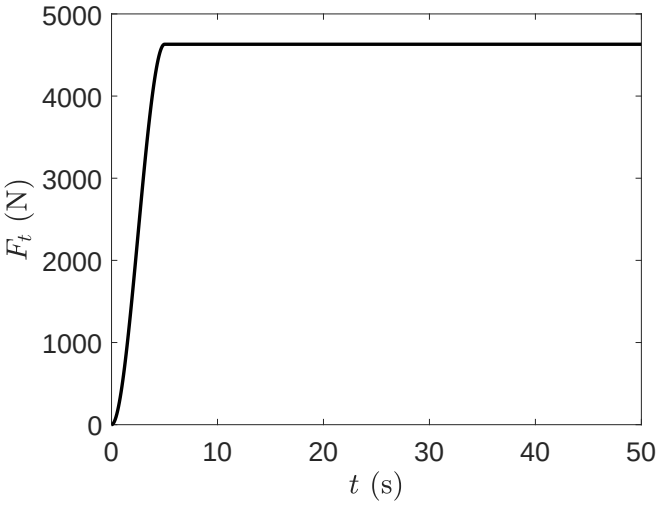

Fig. 3. Thrust force modeled as a ramp function.

denoted with $\mathbf{F}_{n_1}$ associated with the first wheel is given by:

$$\bar{\mathbf{F}}_{n_1} = \begin{bmatrix} 0 \\ F_{n_{c_1}} \end{bmatrix} \tag{26}$$

where:

$$\begin{aligned}\mathbf{F}_{n_1} &= \mathbf{A}_{be} \bar{\mathbf{F}}_{n_1} \\ &= \begin{bmatrix} \cos(\theta) & -\sin(\theta) \\ \sin(\theta) & \cos(\theta) \end{bmatrix} \begin{bmatrix} 0 \\ F_{n_{c_1}} \end{bmatrix} \\ &= \begin{bmatrix} -F_{n_{c_1}} \sin(\theta) \\ F_{n_{c_1}} \cos(\theta) \end{bmatrix}\end{aligned} \tag{27}$$

and

$$F_{n_{c_1}} = \begin{cases} 0 & , \quad z_{c_1} > 0 \\ k z_{c_1} + \sigma \dot{z}_{c_1} & , \quad z_{c_1} \le 0 \end{cases} \tag{28}$$

The second global force vector denoted with $\mathbf{F}_{n_2}$ associated with the second wheel is given by:

$$\bar{\mathbf{F}}_{n_2} = \begin{bmatrix} 0 \\ F_{n_{c_2}} \end{bmatrix} \tag{29}$$

where:

$$\begin{aligned}\mathbf{F}_{n_2} &= \mathbf{A}_{be} \bar{\mathbf{F}}_{n_2} \\ &= \begin{bmatrix} \cos(\theta) & -\sin(\theta) \\ \sin(\theta) & \cos(\theta) \end{bmatrix} \begin{bmatrix} 0 \\ F_{n_{c_2}} \end{bmatrix} \\ &= \begin{bmatrix} -F_{n_{c_2}} \sin(\theta) \\ F_{n_{c_2}} \cos(\theta) \end{bmatrix}\end{aligned} \tag{30}$$

and

$$F_{n_{c_2}} = \begin{cases} 0 & , \quad z_{c_2} > 0 \\ k z_{c_2} + \sigma \dot{z}_{c_2}, & z_{c_2} \le 0 \end{cases} \tag{31}$$

where k and σ are two physical parameters having constant values used to mathematically describe in a simple manner the elastic and dissipative properties of the ground, while z_{c_1}, z_{c_2}, $\dot{z}_{c_1}$, and $\dot{z}_{c_2}$ represent the vertical positions and the vertical velocities of the two points, respectively denoted with W_1 and W_2, at which the contact of the aircraft wheels with the ground occurs.

The aerodynamic actions acting on the system are the lift

force indicated with the vector symbol $\mathbf{L}$, the drag force indicated with the vector symbol $\mathbf{D}$, and the pitching moment indicated with the scalar symbol M_m. The aerodynamic forces (lift and drag) are mathematically defined in the wind-fixed reference system. To correctly project them, a special rotation matrix denoted with $\mathbf{A}_{wb}$ containing the angle of attack is introduced. To this end, in the case of the aerodynamic lift force, one can write:

$$\bar{\mathbf{L}} = \begin{bmatrix} 0 \\ F_L \end{bmatrix} \tag{32}$$

and

$$\begin{aligned} \mathbf{L} &= \mathbf{A}_{be}\mathbf{A}_{wb}\bar{\mathbf{L}} \\ &= \begin{bmatrix} \cos(\theta) & -\sin(\theta) \\ \sin(\theta) & \cos(\theta) \end{bmatrix} \begin{bmatrix} \cos(\alpha) & -\sin(\alpha) \\ \sin(\alpha) & \cos(\alpha) \end{bmatrix} \begin{bmatrix} 0 \\ F_L \end{bmatrix} \end{aligned} \tag{33}$$

Similarly, in the case of the aerodynamic drag force, one can write:

$$\bar{\mathbf{D}} = \begin{bmatrix} -F_D \\ 0 \end{bmatrix} \tag{34}$$

and

$$\begin{aligned} \mathbf{D} &= \mathbf{A}_{be}\mathbf{A}_{wb}\bar{\mathbf{D}} \\ &= \begin{bmatrix} \cos(\theta) & -\sin(\theta) \\ \sin(\theta) & \cos(\theta) \end{bmatrix} \begin{bmatrix} \cos(\alpha) & -\sin(\alpha) \\ \sin(\alpha) & \cos(\alpha) \end{bmatrix} \begin{bmatrix} -F_D \\ 0 \end{bmatrix} \end{aligned} \tag{35}$$

being:

$$F_L = \frac{1}{2}\rho C_L v_{CM,\text{relative}}^2 S \tag{36}$$

$$F_D = \frac{1}{2}\rho C_D v_{CM,\text{relative}}^2 S \tag{37}$$

$$M_m = \frac{1}{2}\rho C_m v_{CM,\text{relative}}^2 Sc \tag{38}$$

where F_L is the intensity of the lift force, F_D is the intensity of the drag force, and M_m is the intensity of the pitching moment.

The kinetic energy of the aircraft system is given by the sum of a translational component and a rotational component as follows:

$$\begin{aligned} T_{\text{aircraft}} &= \tfrac{1}{2}mv_{CM,\text{relative}}^2 + \tfrac{1}{2}I_{yy}\omega_a^2 \\ &= \tfrac{1}{2}m\left(\left(\dot{x} - w_0\cos(\alpha_w)\right)^2 + \left(\dot{z} - w_0\sin(\alpha_w)\right)^2\right) \\ &\quad + \tfrac{1}{2}I_{yy}\dot{\theta}^2 \end{aligned} \tag{39}$$

where m and I_{yy} respectively represent the mass and the mass moment of inertia of the aircraft model. The potential energy of the aircraft system is due to the gravity field and is given by:

$$U_{\text{aircraft}} = mgh_{CM} = mgz \tag{40}$$

By using a Lagrangian approach, the inertia generalized force vector denoted with $\mathbf{Q}_i$ can be systematically obtained using the Lagrange equations of the second kind as follows:

$$\left(\frac{\partial T_{\text{aircraft}}}{\partial \mathbf{q}}\right)^T = \begin{bmatrix} \frac{\partial T_{\text{aircraft}}}{\partial x} \\ \frac{\partial T_{\text{aircraft}}}{\partial z} \\ \frac{\partial T_{\text{aircraft}}}{\partial \theta} \end{bmatrix} = \begin{bmatrix} 0 \\ 0 \\ 0 \end{bmatrix} \tag{41}$$

$$\left(\frac{\partial T_{\text{aircraft}}}{\partial \dot{\mathbf{q}}}\right)^T = \begin{bmatrix} \frac{\partial T_{\text{aircraft}}}{\partial \dot{x}} \\ \frac{\partial T_{\text{aircraft}}}{\partial \dot{z}} \\ \frac{\partial T_{\text{aircraft}}}{\partial \dot{\theta}} \end{bmatrix} = \begin{bmatrix} m\left(\dot{x} - w_0\cos(\alpha)\right) \\ m\left(\dot{z} - w_0\sin(\alpha)\right) \\ I_{yy}\dot{\theta} \end{bmatrix} \tag{42}$$

$$\mathbf{Q}_i = -\frac{d}{dt}\left(\frac{\partial T_{\text{aircraft}}}{\partial \dot{\mathbf{q}}}\right)^T + \left(\frac{\partial T_{\text{aircraft}}}{\partial \mathbf{q}}\right)^T = \begin{bmatrix} -m\ddot{x} \\ -m\ddot{z} \\ -I_{yy}\ddot{\theta} \end{bmatrix} \tag{43}$$

The corresponding mass matrix denoted with $\mathbf{M}$ is given by:

$$\mathbf{M} = -\frac{\partial \mathbf{Q}_i}{\partial \ddot{\mathbf{q}}} = \begin{bmatrix} m & 0 & 0 \\ 0 & m & 0 \\ 0 & 0 & I_{yy} \end{bmatrix} \tag{44}$$

The inertia quadratic velocity vector denoted with $\mathbf{Q}_v$ is given by:

$$\mathbf{Q}_v = \left(\frac{\partial T}{\partial \mathbf{q}}\right)^T - \dot{\mathbf{M}}\dot{\mathbf{q}} = \mathbf{Q}_i + \mathbf{M}\ddot{\mathbf{q}} = \begin{bmatrix} 0 \\ 0 \\ 0 \end{bmatrix} \tag{45}$$

The conservative external generalized force vector indicated with the mathematical symbol $\mathbf{Q}_{e,c}$ can be readily computed as follows:

$$\mathbf{Q}_{e,c} = -\left(\frac{\partial U}{\partial \mathbf{q}}\right)^T = \begin{bmatrix} 0 \\ -mg \\ 0 \end{bmatrix} \tag{46}$$

The total nonconservative external generalized force vector indicated with the mathematical symbol $\mathbf{Q}_{e,nc}$ is, therefore, given by:

$$\begin{aligned} \mathbf{Q}_{e,nc} &= \left(\frac{\delta W_{e,nc}}{\delta \mathbf{q}}\right) \\ &= \mathbf{Q}_{F_p} + \mathbf{Q}_{F_{n1}} + \mathbf{Q}_{F_{n2}} + \mathbf{Q}_L + \mathbf{Q}_D \end{aligned} \tag{47}$$

where $\mathbf{Q}_{F_p}$, $\mathbf{Q}_{F_{n1}}$, $\mathbf{Q}_{F_{n2}}$, $\mathbf{Q}_L$, and $\mathbf{Q}_D$ respectively represent the generalized force vectors associated with the thrust force, the reaction forces of the wheels, and the lift and drag aerodynamic actions, which are respectively given by:

$$\begin{aligned} \mathbf{Q}_T &= \mathbf{L}^T(P)\,\mathbf{F}_P \\ &= \begin{bmatrix} \mathbf{I} \\ \bar{\mathbf{u}}_T^T(P)\,\mathbf{A}_{be}^T \end{bmatrix} \mathbf{F}_P = \begin{bmatrix} \mathbf{F}_P \\ M_T \end{bmatrix} \end{aligned} \tag{48}$$

$$\begin{aligned} \mathbf{Q}_{F_{n_1}} &= \mathbf{L}^T(P)\,\mathbf{F}_{n_1} \\ &= \begin{bmatrix} \mathbf{I} \\ \bar{\mathbf{u}}_{F_{n_1}}^T(P)\,\mathbf{A}_{be}^T \end{bmatrix} \mathbf{F}_{n_1} = \begin{bmatrix} F_{n_1} \\ M_{F_{n_1}} \end{bmatrix} \end{aligned} \tag{49}$$

$$\begin{aligned} \mathbf{Q}_{F_{n_2}} &= \mathbf{L}^T(P)\,\mathbf{F}_{n_2} \\ &= \begin{bmatrix} \mathbf{I} \\ \bar{\mathbf{u}}_{F_{n_2}}^T(P)\,\mathbf{A}_{be}^T \end{bmatrix} \mathbf{F}_{n_2} = \begin{bmatrix} F_{n_2} \\ M_{F_{n_2}} \end{bmatrix} \end{aligned} \tag{50}$$

$$\mathbf{Q}_L = \mathbf{L}^T(P)\,\mathbf{L} = \begin{bmatrix} \mathbf{I} \\ 0 \end{bmatrix} \mathbf{L} = \begin{bmatrix} \mathbf{L} \\ 0 \end{bmatrix} \tag{51}$$

$$\mathbf{Q}_D = \mathbf{L}^T(P)\,\mathbf{D} = \begin{bmatrix} \mathbf{I} \\ 0 \end{bmatrix} \mathbf{D} = \begin{bmatrix} \mathbf{D} \\ 0 \end{bmatrix} \tag{52}$$

The total external generalized force vector denoted with $\mathbf{Q}_e$ applied on the aircraft system is:

$$\mathbf{Q}_e = \mathbf{Q}_{e,c} + \mathbf{Q}_{e,nc} \tag{53}$$

The total body generalized force vector denoted with $\mathbf{Q}_b$ is:

$$\mathbf{Q}_b = \mathbf{Q}_v + \mathbf{Q}_e \tag{54}$$

By using a Lagrangian approach, one can derive the system dynamical model represented in matrix form by the following set of equations of motion:

$$\mathbf{M}\ddot{\mathbf{q}} = \mathbf{Q}_b \tag{55}$$

The set of differential equations obtained in this study for describing the dynamical behavior of the aircraft assumed as the case study is a nonlinear set of Ordinary Differential Equations (ODEs). In the MATLAB simulation environment, these dynamic equations can be analytically implemented and numerically solved through the development of a special-purpose computer code, as shown below in this manuscript.

B. Presentation of the Numerical Results with Simplified Aerodynamics

In this subsection, the numerical results derived in this work in the presence of a preliminary model having simplified aerodynamics are presented. For this purpose, it is assumed that aerodynamic coefficients depend only on the angle of attack, which is mathematically indicated in the paper with the symbol α. Additionally, to cope with the other simplifying hypothesis taken into account in this investigation, it is assumed that the remaining parameters characterizing the dynamical model of the aircraft stay constant during the dynamical simulations. In particular, their numerical values are fixed to the constant value obtained setting to zero the value of the angle of attack. The mathematical definition and the subsequent computer implementation of the dynamical equations of motion of the aircraft system, based on the multibody approach, allow for the use of virtual simulations for assessing the system dynamic behavior in different scenarios of engineering interest. For instance, the initial conditions of the aircraft system, which represent fundamental information to simulate the takeoff maneuver, are considered as the following:

$$\mathbf{q}_0 = \begin{bmatrix} x_0 \\ z_0 \\ \theta_0 \end{bmatrix} = \begin{bmatrix} 0 \\ 0 \\ 0 \end{bmatrix} \tag{56}$$

$$\dot{\mathbf{q}}_0 = \begin{bmatrix} \dot{x}_0 \\ \dot{z}_0 \\ \dot{\theta}_0 \end{bmatrix} = \begin{bmatrix} 0 \\ 0 \\ 0 \end{bmatrix} \tag{57}$$

Considering the set of initial conditions mentioned before and the mathematical model of the aircraft system, it is possible to run a large number of computer simulations in MATLAB and obtain the desired numerical results. In particular, three main arrays of numerical results are presented in this subsection, as shown in Figures 4, 5, and 6.

Considering the takeoff maneuver, the time law found for the angle of attack denoted with α and the trajectory resulting for the aircraft center of mass denoted with G are reported herein, as respectively shown in Figures 4(a) and 4(b). Also,

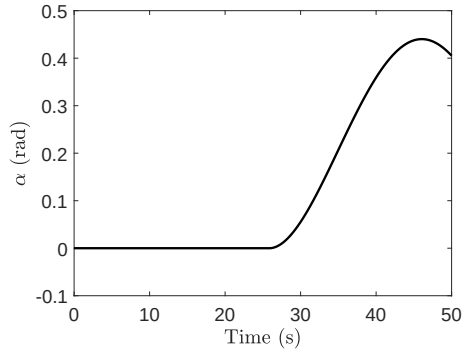

(a) Time evolution of the angle of attack α.

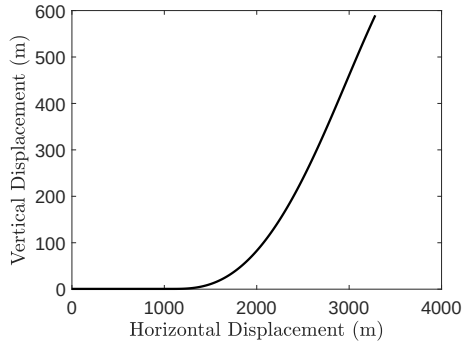

(b) Center of mass $x - z$ trajectory.

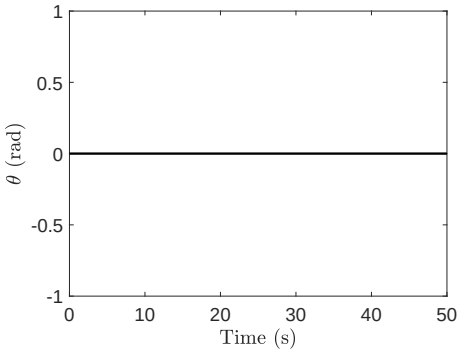

(c) Time evolution of the angular displacement θ.

Fig. 4. Aircraft dynamic behavior with simplified aerodynamics.

Figure 4(c) represents the variation in time of the angle θ. Figures 5(a), 5(b), and 5(c) show the variation in time of the horizontal, vertical, and angular velocity, respectively. Finally, Figure 6(a) shows the time transient of the lift force, Figure 6(b) represents the time transient in time of the drag force, whereas Figure 6(c) represents the time transient of the net pitching moment. From a physical standpoint, the numerical results shown in Figures 4, 5, and 6 are consistent with what is expected for the transient behavior of the aircraft in correspondence of the takeoff maneuver under the simplifying assumptions adopted [84].

C. Presentation of the Numerical Results with Realistic Aerodynamics

In this subsection, the variation of the aerodynamic coefficients is taken into account. Furthermore, the influence of the elevator is considered, which mainly influences the lift coefficient and the pitching moment coefficient. Usually, the deflection of the elevator is defined as positive with

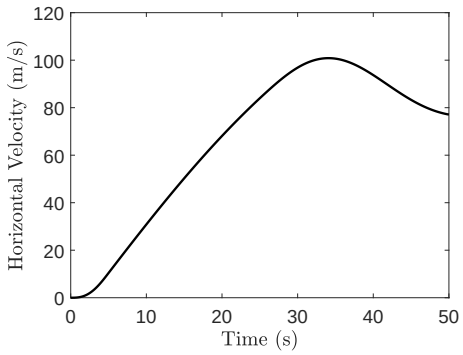

(a) Time evolution of the horizontal velocity.

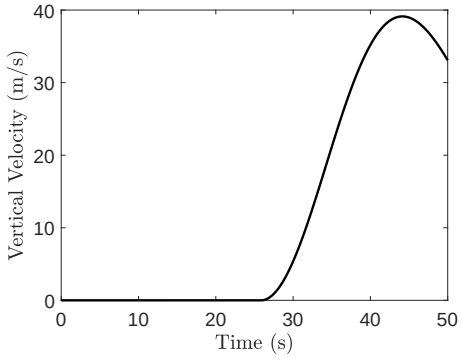

(b) Time evolution of the vertical velocity.

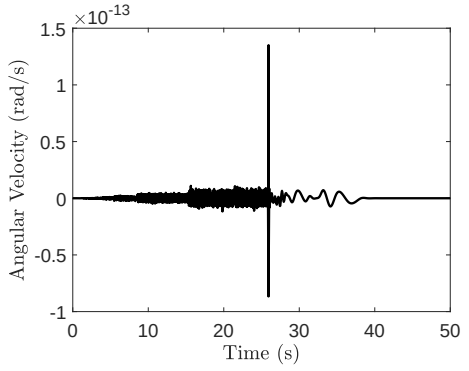

(c) Time evolution of the angular velocity.

Fig. 5. Dynamic behavior of the aircraft velocity with simplified aerodynamics.

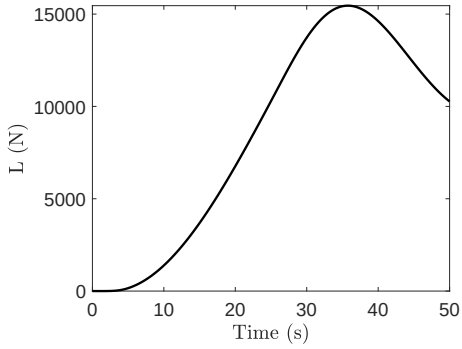

(a) Time evolution of the lift force.

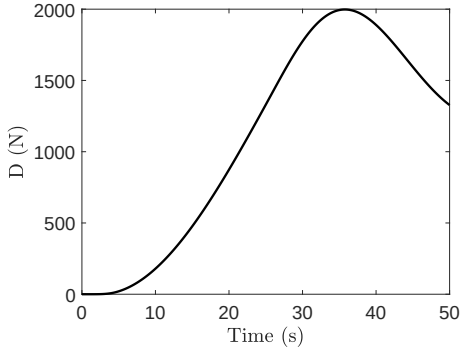

(b) Time evolution of the drag force.

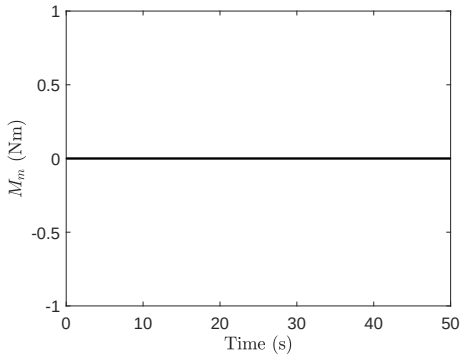

(c) Time evolution of the net pitching moment.

Fig. 6. Dynamic behavior of the aerodynamic actions with simplified aerodynamics.

a downward elevator deflection, negative vice versa. The mathematical expression of the aerodynamic coefficients can be written in the following simplified form:

$$C_L = C_L(\alpha, \delta_e) = C_L^0 + \Delta C_L \tag{58}$$

$$C_D = C_D(\alpha) = C_D^0 \tag{59}$$

$$C_m = C_m(\alpha, \delta_e) = C_m^0 + \Delta C_m \tag{60}$$

where C_L^0, C_D^0, and C_m^0 are the aerodynamic coefficients value in absence of the elevator, whereas ΔC_L and ΔC_m are the variations of the aerodynamic coefficients due to the presence of the deflection of the elevator. These values are obtained through Digital DATCOM, a database based on a collection of experimental test results carried out in the wind tunnel in various configurations and for various aircraft. By compiling the input file for the aircraft considered, an output file is obtained containing, among other information, the numerical values of the aerodynamic coefficients as the angle of attack varies as well as the increases they undergo as the angle of deflection of the elevator. By using the appropriate function, called *datcomimport*, one can import the Digital DATCOM output file in a vector form in MATLAB. The values of the aerodynamic coefficients imported in MATLAB are, therefore, discrete. To transform them into continuous functions, the following polynomial interpolation is used:

$$C_k = C_k^0 + \Delta C_k \tag{61}$$

where C_k depends only on the angle of attack denoted with α and ΔC_k depends only on the deflection of the elevator denoted with δ_e. The interpolating functions associated with the aerodynamic coefficients are defined as follows:

$$C_k^0 = \sum_{i=0}^{N} a_i \alpha^i, \quad \Delta C_k = \sum_{j=0}^{M} b_j \delta_e^j \tag{62}$$

where a_i and b_j are the constant coefficients that appear in the interpolating functions describing the aerodynamic coefficients. The aerodynamic coefficients obtained from the computer implementation of the analysis described above are shown in Figure 7.

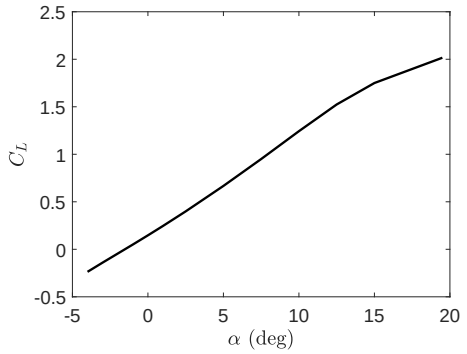

(a) Lift coefficient.

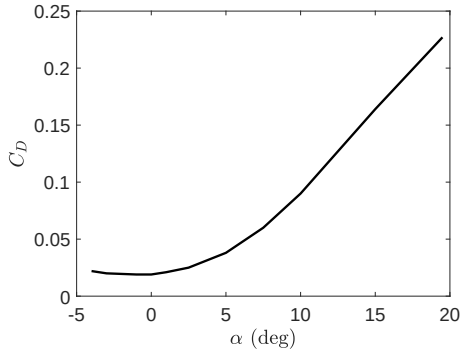

(b) Drag coefficient.

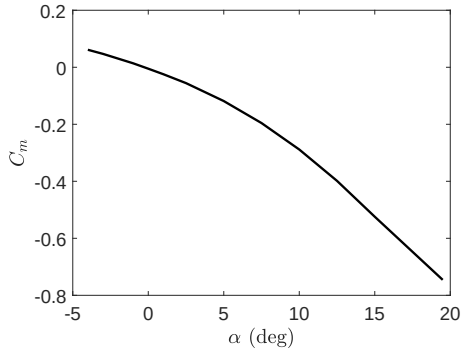

(c) Pitching moment coefficient.

Fig. 7. Polynomial interpolation of the aerodynamic coefficients.

In particular, the variation of the lift coefficient with respect to the angle of attack is shown in Figure 7(a), the variation of the drag coefficient with respect to the angle of attack is shown in Figure 7(b), and the variation of the pitching moment coefficient with respect to the angle of attack is shown in Figure 7(c).

In Figures 8, 9, and 10, on the other hand, the main numerical results obtained from dynamical simulations corresponding to the scenario with more realistic aerodynamics are shown.

More specifically, the variation in time of the angle of attack is represented in Figure 8(a), the global trajectory of the centroid of the aircraft is represented in Figure 8(b), and the time transient of the angle θ is represented in Figure

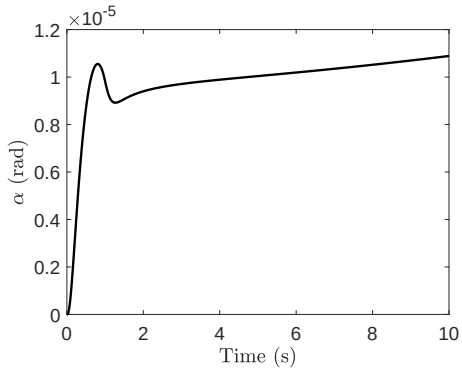

(a) Time evolution of the angle of attack α.

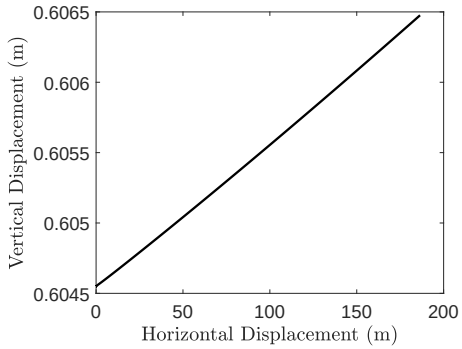

(b) Center of mass $x - z$ trajectory.

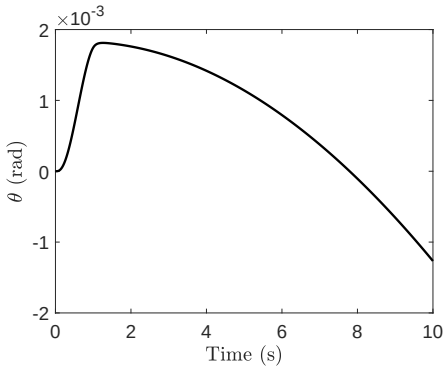

(c) Time evolution of the angular displacement θ.

Fig. 8. Aircraft dynamic behavior with more realistic aerodynamics.

8(c). Additionally, Figures 9(a), 9(b), and 9(c) show the time transient of the vertical, horizontal, and angular velocity, respectively. Finally, Figure 10(a) represents the time transient of the lift force, Figure 10(b) represents the time transient of the drag force, while Figure 10(c) represents the time transient of the net pitching moment. Again, the transient behavior of the Cessna aircraft system that is assumed as the demonstrative example of the present paper is in full agreement with the physics of the problem under study.

D. Remarks and Discussion

This subsection proposes some general remarks and a short discussion about the dynamical behavior of the aircraft system assumed as the demonstrative example of the paper. More precisely, some comments about the accuracy of the numerical results obtained through dynamic simulations are reported herein. In general, despite the simplifying hypothesis necessary for reasonably modeling the aircraft system

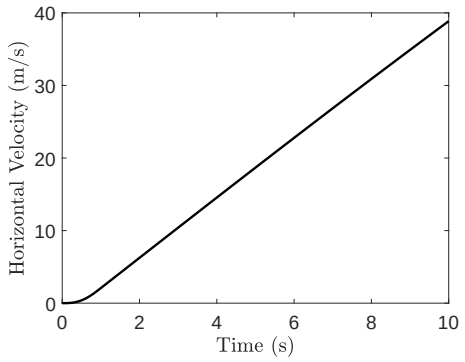

(a) Time evolution of the horizontal velocity.

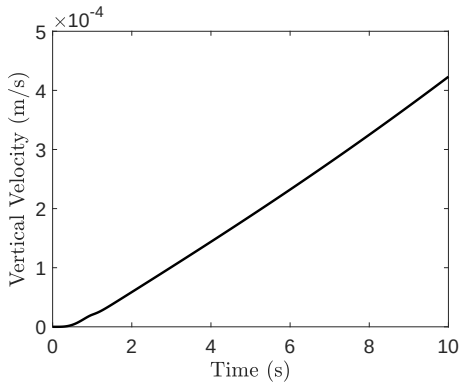

(b) Time evolution of the vertical velocity.

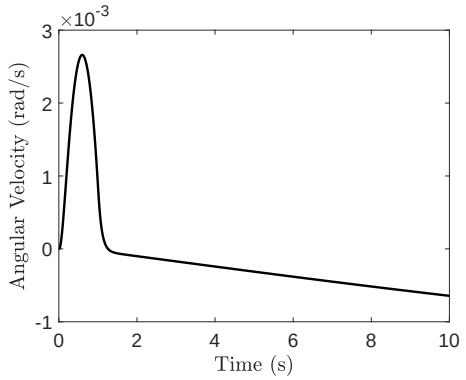

(c) Time evolution of the angular velocity.

Fig. 9. Dynamic behavior of the aircraft velocity with more realistic aerodynamics.

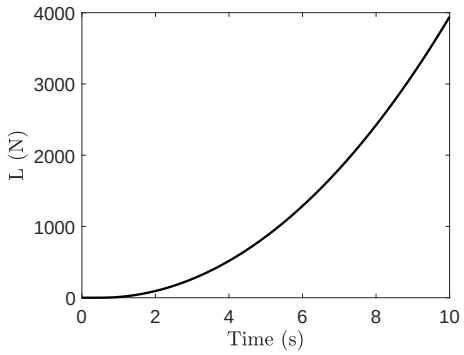

(a) Time evolution of the lift force.

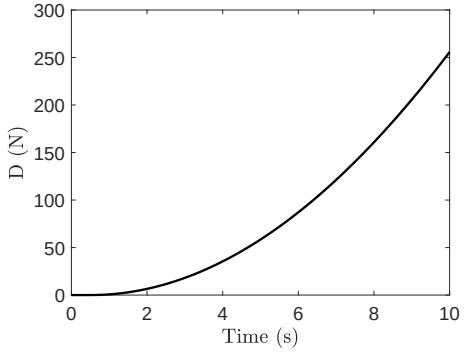

(b) Time evolution of the drag force.

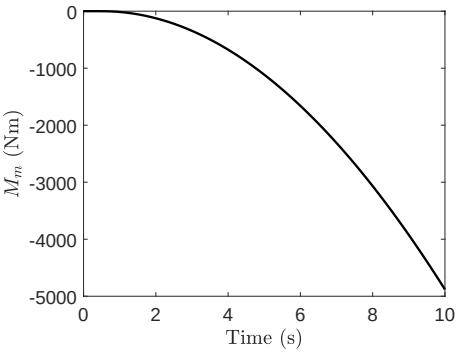

(c) Time evolution of net pitching moment M_m.

Fig. 10. Dynamic behavior of the aerodynamic actions with more realistic aerodynamics.

representing the case study, it can be stated that the desired motion of the aircraft system during the takeoff phase was correctly reproduced using the computer simulations carried out in the MATLAB environment.

With respect to the first simulation, consistently with the simplified assumptions adopted, the angle denoted with θ assumes zero value along with the entire simulation, as well as the pitching moment. In accordance with the characteristics of the aircraft system considered in the case study, the detachment from the ground takes place after around 30 seconds. Another fundamental aspect is relative to the time transient of the angle of attack, which is indicated by the symbol α. Initially, the angle of attack is almost identically equal to zero. As the altitude of the aircraft increases, the numerical value of the angle of attack starts growing in correspondence with the ground run. Subsequently, one can observe that the angle of attack decrease when it reaches a certain value of about 0.45 radians, and this behavior could be explained by imagining that the stall phenomenon starts taking place since the value of the angle of attack is becoming too high. The triggering of the stall phenomenon leads to a sudden and sharp reduction of the value of the lift force, and, at the same time, a drastic increase in the value of the drag force. The final result is, therefore, a reduction of the vertical altitude of the aircraft, thereby representing a dangerous situation to be avoided [85]–[88]. To timely counteract this problem and to avoid excessive growth of the absolute value of the angle of attack, the pilot and/or the aircraft control system must properly adjust the deflection of the control surfaces to properly guide the motion of the aircraft [89], [90].

With respect to the results obtained from the second simulation, making a comparison with the results obtained from the first simulation, it can be seen how the presence of the elevator generates greater values of the magnitudes of

the lift force as well as of the pitching moment. However, it is particularly important to note that the altitude of the aircraft does not increase excessively during the simulation time. This is due to the fact that modeling the thrust force as a ramp function and imposing a constant deflection of the elevator are not sufficient assumptions to effectively control the system. Therefore, it would be more appropriate to model the deflection of the elevator as an explicit function of time. Furthermore, the aircraft system is under-actuated as one wants to control three output variables, namely two linear displacements and one angular displacement, by manipulating only two input variables, namely the thrust force and the deflection of the elevator. These important aspects were not deliberately considered in this investigation and will be addressed in future works.

IV. Summary, Conclusions, and Future Work

In general, the authors are interested in three main research fields concerning multibody dynamics, nonlinear control, and applied identification of mechanical systems. More specifically, these research areas are system identification of structural systems, control of robotic manipulators, and rigid-flexible dynamics of articulated mechanisms [91]–[95]. This paper fits this research framework because it is devoted to the development of a simplified model for the longitudinal flight dynamics of the aircraft called Cessna 172 Skyhawk. This objective is achieved within the multibody system framework and employing a fully Lagrangian approach for the mathematical generation of equations of motion, which is subsequently implemented and solved by using MATLAB computer codes specifically developed by the authors.

In summary, under appropriate simplifying assumptions, a multibody model that can correctly simulate the longitudinal dynamics of an aircraft was developed in this paper. To consistently capture the geometry, inertia, and aerodynamic properties of the system of interest for this investigation, the illustrative system analyzed in this study is the Cessna 172 Skyhawk. In order to focus on the longitudinal flight dynamics, the aircraft under consideration was modeled as a multibody system endowed only with a planar motion, that is, only three degrees of freedom were considered in the virtual model, while the externally applied forces were assumed to be applied following a simplified configuration. A comprehensive computer code, programmed in MATLAB to numerically solve the multibody equations of motions that were mathematically derived in the paper, was used to carry out the necessary virtual simulations considering a Lagrangian formulation. For this purpose, in the last version of the simplified aircraft model devised in this study, a realistic set of aerodynamic coefficients obtained from the digital DATCOM software is used to perform dynamic simulations. The computational results obtained in this work through numerical simulations realized in the MATLAB simulation environment are consistent with the physics behind the problem at hand.

In future research works, the goal is to consider not only the action of the control surfaces but also the dynamics of the aircraft in a three-dimensional space, thereby enhancing the basic description of the aircraft and removing the simplifying assumptions taken into account in this preliminary study. In this vein, the authors want to derive in the multibody framework a more sophisticated mathematical model of the aircraft considered as the illustrative example of the present paper having six degrees of freedom. The modeling of the aerodynamic coefficients should be improved as well in future investigations employing, for example, a combination of the information obtained using the digital DATCOM software with the theory that stands behind the vortex lattice method. Also, by considering a more comprehensive dynamical model, in future investigations will be possible to explore the topic of aircraft control by modeling the deflection of the elevator and the other control surfaces, as well as the thrust as a specifically designed function of time. In future investigations, the relevant topics mentioned before will be fully addressed and thoroughly explored.

Authors' Contributions

This research paper was principally devised and developed by the first author (Carmine Maria Pappalardo). Great support in the development of this work was provided by the second author (Maria Curcio). The detailed review carried out by the third author (Domenico Guida) considerably improved the quality of the manuscript. The manuscript was written with the contribution of all authors. All authors discussed the results, reviewed the methodology, and approved the final version of the manuscript.

References

[1] F. Villecco, "On the evaluation of errors in the virtual design of mechanical systems," *Machines*, vol. 6, no. 3, 36, 2018.

[2] Y. Gao, F. Villecco, M. Li, and W. Song, "Multi-scale permutation entropy based on improved LMD and HMM for rolling bearing diagnosis," *Entropy*, vol. 19, no. 4, 176, 2017.

[3] J. Li, and C. Liu, "A class of polynomial spline curve with free parameters that naturally interpolates the data points," *IAENG International Journal of Applied Mathematics*, vol. 50, no. 3, pp643-647, 2020.

[4] S. Ardila-Parra, C. Pappalardo, O. Estrada, and D. Guida, "Finite element based redesign and optimization of aircraft structural components using composite materials," *IAENG International Journal of Applied Mathematics*, vol. 50, no. 4, pp860-877, 2020.

[5] C. Manrique Escobar, C. Pappalardo, and D. Guida, "A parametric study of a deep reinforcement learning control system applied to the swing-up problem of the cart-pole," *Applied Sciences*, vol. 10, no. 24, 9013, 2020.

[6] C. Pappalardo, A. Manca, and D. Guida, "A combined use of the multibody system approach and the finite element analysis for the structural redesign and the topology optimization of the latching component of an aircraft hatch door," *IAENG International Journal of Applied Mathematics*, vol. 51, no. 1, pp175-191, 2021.

[7] N. Sinha, and N. Ananthkrishnan, "Elementary flight dynamics with an introduction to bifurcation and continuation methods," *CRC Press*, 2021.

[8] A. Vuruskan, B. Yuksek, U. Ozdemir, A. Yukselen, and G. Inalhan, "Dynamic modeling of a fixed-wing VTOL UAV," *2014 International Conference On Unmanned Aircraft Systems (ICUAS)*, IEEE, pp483-491, 2014.

[9] N. Sinha, and N. Ananthkrishnan, "Advanced flight dynamics with elements of flight control," *CRC Press*, 2017.

[10] T. Gleason, "Introduction to UAV systems," *Wiley*, 2012.

[11] R. Beard, and T. McLain, "Small unmanned aircraft: theory and practice," *Small Unmanned Aircraft*, Princeton university press, 2012.

[12] M. Sghairi, A. De Bonneval, Y. Crouzet, J. Aubert, and P. Brot, "Challenges in Building Fault-Tolerant Flight Control System for a Civil Aircraft," *IAENG International Journal of Computer Science*, vol. 35, no. 4, pp495-499, 2008.

[13] Q. Quan, "Introduction to multicopter design and control," *Springer*, 2017.

[14] Q. Quan, X. Dai,and S. Wang, "Multicopter design and control practice: a series experiments based on MATLAB and Pixhawk," *Springer Nature*, 2020.

[15] M. Lopez-Rivera, A. Cortes-Villada, and E. Giraldo, "Optimal multivariable control design based on a fuzzy model for an unmanned aerial vehicle," *IAENG International Journal of Computer Science*, vol. 48, no. 2, pp316-321, 2021.

[16] M. Sadraey, "Design of unmanned aerial systems," *John Wiley & Sons*, 2020.

[17] M. De Simone, and D. Guida, "Control design for an under-actuated UAV model," *FME Transactions*, vol. 46, no. 4, pp443-452, 2018.

[18] G. Capitta, L. Damiani, S. Laudani, E. Lertora, C. Mandolfino, E. Morra, and R. Revetria, "Structural and operational design of an innovative airship drone for natural gas transport over long distances," *Engineering Letters*, vol. 25, no. 3, pp247-254, 2017.

[19] H. Shakhatreh, A. Sawalmeh, A. Al-Fuqaha, Z. Dou, E. Almaita, I. Khalil, N. Othman, A. Khreishah, and M. Guizani, "Unmanned aerial vehicles (UAVs): a survey on civil applications and key research challenges," *IEEE Access*, vol. 7, pp48572-48634, 2019.

[20] Y. Sebbane, "A first course in aerial robots and drones," *CRC Press*, 2022.

[21] D. Bai, J. Tian, D. Li, and S. Li, "Multiple UAVs tracking for moving ground target," *Engineering Letters*, vol. 30, no. 2, pp829-834, 2022.

[22] L. Belmonte, R. Morales, and A. Fernández-Caballero, "Computer vision in autonomous unmanned aerial vehicles - a systematic mapping study," *Applied Sciences*, vol. 9, no. 15, 3196, 2019.

[23] J. Choi, R. Curry, and G. Elkaim, "Continuous curvature path generation based on Bézier curves for autonomous vehicles," *IAENG International Journal of Applied Mathematics*, vol. 40, no. 2, pp91-101, 2010.

[24] M. Cifuentes-Molano, B. Hernandez, and E. Giraldo, "Comparison of different control techniques on a bipedal robot of 6 degrees of freedom," *IAENG International Journal of Applied Mathematics*, vol. 51, no. 2, pp300-306, 2021.

[25] A. Nagendran, W. Crowther, and R. Richardson, "Biologically inspired legs for UAV perched landing" *IEEE Aerospace And Electronic Systems Magazine*, vol. 27, no. 2, pp4-13, 2012.

[26] A. Shabana, "Dynamics of multibody systems," *Cambridge university press*, 2003.

[27] A. Shabana, "Computational Dynamics," *John Wiley & Sons*, 2009.

[28] A. Shabana, "Computational continuum mechanics," *John Wiley & Sons*, 2018.

[29] A. Shabana, "Integration of computer-aided design and analysis: application to multibody vehicle systems," *International Journal of Vehicle Performance*, vol. 5, no. 3, pp300-327, 2019.

[30] A. Mikkola, A. Shabana, C. Sanchez-Rebollo, and J. Jimenez-Octavio, "Comparison between ANCF and B-spline surfaces," *Multibody System Dynamics*, vol. 30, n. 2, pp119-138, 2013.

[31] G. Orzechowski, M. Matikainen, and A. Mikkola, "Inertia forces and shape integrals in the floating frame of reference formulation," *Nonlinear Dynamics*, vol. 88, no. 3, pp1953-1968, 2017.

[32] M. Muscat, A. Cammarata, P. Maddio, and R. Sinatra, "Design and development of a towfish to monitor marine pollution," *Euro-Mediterranean Journal For Environmental Integration*, vol. 3, no. 1, 11, 2018.

[33] T. Tanev, A. Cammarata, D. Marano, and R. Sinatra, "Elastostatic model of a new hybrid minimally-invasive-surgery robot," *The 14th IFToMM World Congress*, Taipei, Taiwan, 2015.

[34] H. Goldstein, C. Poole, and J. Safko, "Classical mechanics," *American Association of Physics Teachers*, 2002.

[35] L. Meirovitch, "A new modal method for the response of structures rotating in space," *Acta Astronautica*, vol. 2, no. 7-8, pp563-576, 1975.

[36] M. Waszak, and D. Schmidt, "Flight dynamics of aeroelastic vehicles," *Journal of Aircraft*, vol. 25, no. 6, pp563-571, 1988.

[37] G. Avanzini, E. Capello, and I. Piacenza, "Mixed Newtonian–Lagrangian approach for the analysis of flexible aircraft dynamics," *Journal of Aircraft*, vol. 51, no. 5, pp1410-1421, 2014.

[38] F. Nicassio, D. Fattizzo, M. Giannuzzi, G. Scarselli, and G. Avanzini, "Attitude dynamics and control of a large flexible space structure by means of a minimum complexity model," *Acta Astronautica*, vol. 198, pp124-134, 2022.

[39] N. Peyada, and A. Ghosh, "Aircraft parameter estimation using a new filtering technique based upon a neural network and Gauss-Newton method," *The Aeronautical Journal*, vol. 113, no. 1142, pp243-252, 2009.

[40] J. Thelander, "Aircraft motion analysis," *Douglas Aircraft CO Long Beach CA*, Tech. Rep., 1965.

[41] B. Mukherjee, and M. Sinha, "Nonlinear dynamics and control of a laterally mass varying fighter aircraft," *Proceedings of The Institution of Mechanical Engineers, Part G: Journal of Aerospace Engineering*, vol. 232, no. 16, pp3118-3134, 2018.

[42] B. Mukherjee, and M. Sinha, "Large angle maneuvering with an asymmetric aircraft: a single loop control formulation," *2018 AIAA Guidance, Navigation, And Control Conference*, 1869, 2018.

[43] Y. Tu, and G. Lin, "Dynamic simulation of aircraft environmental control system based on flowmaster," *Journal of Aircraft*, vol. 48, no. 6, pp2031-2041, 2011.

[44] F. Yang, and X. Yuan, "Matlab-based dynamic simulation of aircraft environmental control system," *Acta Simulata Systematica Sinica*, vol. 14, no. 6, pp782-785, 2002.

[45] B. Mukherjee, and M. Sinha, "A single loop dynamic inversion control for a fighter aircraft executing rapid large amplitude maneuvers," *2017 14th IEEE India Council International Conference (INDICON)*, 8487772, 2017.

[46] D. Rao, and N. Sinha, "Aircraft spin recovery using a sliding-mode controller," *Journal of Guidance, Control, And Dynamics*, vol. 33, no. 5, pp1675-1679, 2010.

[47] J. Trachte, L. Toro, and A. McFadyen, "Multi-rotor with suspended load: System dynamics and control toolbox," *2015 IEEE Aerospace Conference*, 7119210, 2015.

[48] K. Harikumar, J. Senthilnath, and S. Sundaram, "Multi-UAV oxyrrhis marina-inspired search and dynamic formation control for forest firefighting," *IEEE Transactions On Automation Science And Engineering*, vol. 16, no. 2, pp863-873, 2018.

[49] R. Jategaonkar, "Flight vehicle system identification: a time domain methodology," *American Institute of Aeronautics*, 2006.

[50] C. Pappalardo, A. Lettieri, and D. Guida, "Identification of a dynamical model of the latching mechanism of an aircraft hatch door using the numerical algorithms for subspace state-space system identification," *IAENG International Journal of Applied Mathematics*, vol. 51, no. 2, pp346-359, 2021.

[51] C. Hamel, R. Botez, and M. Ruby, "Cessna citation x airplane grey-box model identification without preliminary data," SAE Technical Paper, Tech. Rep., 2014.

[52] M. Sinha, R. Kuttieri, and S. Chatterjee, "Nonlinear and linear unstable aircraft parameter estimations using neural partial differentiation," *Journal of Guidance, Control, And Dynamics*, vol. 36, no. 4, pp1162-1176, 2013.

[53] A. Cammarata, "Global modes for the reduction of flexible multibody systems," *Multibody System Dynamics*, vol. 53, no. 1, pp59-83, 2021.

[54] E. Pennestrí, P. Valentini, and D. Falco, "An application of the Udwadia–Kalaba dynamic formulation to flexible multibody systems," *Journal of The Franklin Institute*, vol. 347, no. 1, pp173-194, 2010.

[55] D. Negrut, A. Tasora, H. Mazhar, T. Heyn, and P. Hahn, "Leveraging parallel computing in multibody dynamics," *Multibody System Dynamics*, vol. 27, no. 1, pp95-117, 2012.

[56] L. Cavagna, P. Masarati, and G. Quaranta, "Coupled multibody/computational fluid dynamics simulation of maneuvering flexible aircraft," Journal of Aircraft, vol. 48, no. 1, pp92-106, 2011.

[57] C. Pappalardo, and D. Guida, "On the computational methods for solving the differential-algebraic equations of motion of multibody systems," *Machines*, vol. 6, no. 2, 20, 2018.

[58] C. Manrique-Escobar, C. Pappalardo, and D. Guida, "A multibody system approach for the systematic development of a closed-chain kinematic model for two-wheeled vehicles," *Machines*, vol. 9, no. 11, 245, 2021.

[59] E. Leylek, M. Ward, and M. Costello, "Flight dynamic simulation for multibody aircraft configurations," *Journal of Guidance, Control, And Dynamics*, vol. 35, no. 6, pp1828-1842, 2012.

[60] M. Castellani, J. Cooper, and Y. Lemmens, "Flight loads prediction of high aspect ratio wing aircraft using multibody dynamics," *International Journal of Aerospace Engineering*, vol. 2016, no. 1, 135090, 2016.

[61] Z. Zhao, and G. Ren, "Multibody dynamic approach of flight dynamics and nonlinear aeroelasticity of flexible aircraft," *AIAA Journal*, vol. 49, no. 1, pp41-54, 2011.

[62] V. Bagherian, M. Salehi, and M. Mahzoon, "Rigid multibody dynamic modeling for a semi-submersible wind turbine," *Energy Conversion And Management*, vol. 244, 114399, 2021.

[63] M. Al-Solihat, and M. Nahon, "Flexible multibody dynamic modeling of a floating wind turbine," *International Journal of Mechanical Sciences*, vol. 142, pp518-529, 2018.

[64] C. Manrique-Escobar, C. Pappalardo, and D. Guida, "On the analytical and computational methodologies for modelling two-wheeled vehicles within the multibody dynamics framework: a systematic literature review," *Journal of Applied And Computational Mechanics*, vol. 8, no. 1, pp153-181, 2022.

[65] N. Ananthkrishnan, and N. Sinha, "A simple, correct pedagogical presentation of airplane longitudinal dynamics," *AIAA Atmospheric Flight Mechanics (AFM) Conference*, 4740, 2013.

[66] A. Cammarata, M. Lacagnina, and R. Sinatra, "Closed-form solutions for the inverse kinematics of the Agile Eye with constraint errors on the revolute joint axes," *2016 IEEE/RSJ International Conference On Intelligent Robots And Systems (IROS)*, pp317-322, 2016.

[67] Z. Huang, F. Xi, T. Huang, J. Dai, and R. Sinatra, "Lower-mobility parallel robots: theory and applications," *Advances In Mechanical Engineering*, vol. 2, 927930, 2010.
[68] A. Cammarata, R. Sinatra, A. Rigano, M. Lombardo, and P. Maddio, "Design of a large deployable reflector opening system," *Machines*, vol. 8, no. 1, 7, 2020.
[69] C. Kim, "Scale modeling of Cessna 172," *American Institute of Aeronautics and Astronautics*, 2011.
[70] R. Smith, "Cessna 172: a pocket history," *Amberley Publishing Limited*, 2010.
[71] L. Meirovitch, "Computational methods in structural dynamics," *Springer Science & Business Media*, vol. 5, 1980.
[72] M. Ardema, "Analytical dynamics: theory and applications", New York, Boston, Dordrecht, London, *Moscow: Klwer Acanemic*, Plenum Publishers, 2005.
[73] W. Schiehlen, "Multibody system dynamics: roots and perspectives," *Multibody System Dynamics*, vol. 1, no. 2, pp149-188, 1997.
[74] L. Mariti, N. Belfiore, E. Pennestrí, and P. Valentini, "Comparison of solution strategies for multibody dynamics equations," *International Journal For Numerical Methods In Engineering*, vol. 88, no. 7, pp637-656, 2011.
[75] L. Meirovitch, "Methods of analytical dynamics," Courier Corporation, 2010.
[76] J. Papastavridis, and K. Yagasaki, "Analytical mechanics: a comprehensive treatise on the dynamics of constrained systems; for engineers, physicists, and mathematicians," *Applied Mechanics Review*, vol. 56, no. 2, pp1-1392, 2003.
[77] B. Dillman, D. Wilt, S. Pruchnicki, and T. Hall, "Effect of angle of attack displays on approach stability," *AIAA Atmospheric Flight Mechanics Conference*, 4064, 2017.
[78] W. Frost, and R. Bowles, "Wind shear terms in the equations of aircraft motion" *Journal of Aircraft*, vol. 21, no. 11, pp866-872, 1984.
[79] T. Johansen, A. Cristofaro, K. Sørensen, J. Hansen, and T. Fossen, "On estimation of wind velocity, angle-of-attack and sideslip angle of small UAVs using standard sensors," *2015 International Conference On Unmanned Aircraft Systems (ICUAS)*, pp510-519, 2015.
[80] L. Sankaralingam, and C. Ramprasadh, "A comprehensive survey on the methods of angle of attack measurement and estimation in UAVs," *Chinese Journal of Aeronautics*, vol. 33, no. 3, pp749-770, 2020.
[81] A. Babister, "Aircraft Dynamic Stability and Response" Pergamon International Library of Science, Technology, *Engineering and Social Studies*, Elsevier, 2013.
[82] K. Jackson, and E. Fasanella, "Crash Testing and Simulation of a Cessna 172 Aircraft: Hard Landing Onto Concrete," *International LS-DYNA Conference*, NF1676L-22884, 2016.
[83] M. Acanfora, A. De Marco, and L. Lecce, "Development, Modeling and Simulation of Multiple Design Concepts for a Small Unmanned Airship," *AIAA Modeling And Simulation Technologies Conference*, 6521, 2011.
[84] J. McIver, "Cessna Skyhawk II/100, Performance Assessment", *Temporal Images, Melbourne, Australia*, 2003.
[85] N. Kabir, "Indigenous design of pitch control system of short range aircraft," *Department of Electrical*, 2013.
[86] B. Lierop, "Handling qualities criteria for training effectiveness assessment of the BS115 aircraft," *TU Delft University of Technology*, 2017.
[87] P. Vadivelu, D. Lakshmanan, R. Naveen, K. Mathivannan, and G. Kumar, "Numerical study on longitudinal control of Cessna 172 Skyhawk aircraft by tail arm length," *IOP Conference Series: Materials Science And Engineering*, vol. 764, no. 1, 012026, 2020.
[88] T. Brecht, "Micromachined quantum circuits," *Yale University*, 2017.
[89] M. Guida, A. Manzoni, A. Zuppardi, F. Caputo, F. Marulo, and A. De Luca, "Development of a multibody system for crashworthiness certification of aircraft seat," *Multibody System Dynamics*, vol. 44, no. 2, pp191-221, 2018.
[90] L. Tong, and H. Ji, "Multi-body dynamic modelling and flight control for an asymmetric variable sweep morphing UAV," *The Aeronautical Journal*, vol. 118, no. 1204, pp683-706, 2014.
[91] C. Pappalardo, M. De Simone, and D. Guida, "Multibody modeling and nonlinear control of the pantograph/catenary system," *Archive of Applied Mechanics*, vol. 89, no. 8, pp1589-1626, 2019.
[92] C. Pappalardo, A. Lettieri, and D. Guida, "A general multibody approach for the linear and nonlinear stability analysis of bicycle systems. Part I: Methods of constrained dynamics," *Journal of Applied And Computational Mechanics*, vol. 7, no. 2, pp655-670, 2021.
[93] C. Pappalardo, A. Lettieri, and D. Guida, "A general multibody approach for the linear and nonlinear stability analysis of bicycle systems. Part II: Application to the whipple-carvallo bicycle model," *Journal of Applied And Computational Mechanics*, vol. 7, no. 2, pp671-700, 2021.
[94] C. Pappalardo, and D. Guida, "Dynamic analysis and control design of kinematically-driven multibody mechanical systems," *Engineering Letters*, vol. 28, no. 4, pp1125-1144, 2020.
[95] M. De Simone, and D. Guida, "Modal coupling in presence of dry friction," *Machines*, vol. 6, no. 1, 8, 2018.